

Comments and associated responses for:

Processes influencing heat transfer in the near-surface ice of Greenland's ablation zone

Benjamin H. Hills et al. 2018

Anonymous Referee #2

Author responses are in blue.

Hills et al. Investigate heat transfer from the atmosphere to the ice in west Greenland's ablation zone and conclude based that air temperature can not predict the near-surface ice temperature. While the topic is interesting and the data presented is valuable, the modelling part does not lead to strong conclusions. I would recommend to rework the paper, focus on the data analysis, especially the very interesting transient heating events, ideally deriving quantitative conclusions on the amount of water necessary to reproduce them and modify the modelling part significantly. Some assumptions for the model-part seem inappropriate or at least too weakly constrained in order to judge if the derived conclusions are valid. Comparison with Promice stations in the area may improve the applicability and validate some of the factors. Central is an in-depth check of the boundary (6) for the modelling part. This should be discussed thoroughly. Take a promice station in the area, convert outgoing longwave radiation with Stefan Boltzmann to surface temperature and plot vs air temperature. This plot is necessary for the paper and will show if (6) is OK to use at all. Also, put more effort into explaining the massive local-scale variability of ice temperatures which is surprising to me. Generally, I would suggest major revisions, a change in focus of the paper and/or a substantial improvement of the modelling part.

Thank you for these comments. We appreciate the requested change of focus from the model to the data, and have made a substantial effort to carry out this request. We have removed the emphasis on meteorological data, as both reviewers seemed to get lost in those details and our intention was always to focus on ice temperature and not meteorological processes. We have added explanations of the transient features in the data, and, as requested, have added an analysis of the subsurface refreezing events (Figure 7).

We appreciate that the modeling results are somewhat inconsistent with the data, but we would argue that this is in and of itself a worthwhile conclusion. The processes that we investigate do not account for the measured temperature discrepancy, so some other process not modeled must be important. We have added language to the discussion, emphasizing the importance of the subsurface refreezing events. We state that the measured temperature discrepancy must be either a result of those heating events, or a result of the subsurface temperature gradient being positive because of a deeper energy source.

Finally, to address some of the concerns with the meteorological data, we have added to the supplement. We compare our measurements to those of the KAN_L PROMICE station (Figure S4). We also add a surface ice temperature calculated with the Stefan-Boltzmann Law.

P2 L12: add reference?

Added Cuffey and Paterson (2010).

L19 – if it is often used, add more references. This is potentially an important issue.

Added Mock and Weeks (1966). These are the two most seminal studies (one from Greenland and the other from Antarctica) of this time period around the IGY when this method was used most. We argue that more references would be redundant.

P3 L1: this statement is true for all ablation areas and is not GrIS specific!?

Changed to “the processes which make the ablation zone different from other areas of a glacier or ice sheet”

L7-8. Can observation resolve these processes quantitatively? In my view this is the ‘issue’ with observations, that you end up with a ‘bulk’ signal combining different processes. Consider rewording

Changed paragraph:

“Our near-surface temperature observations represent an aggregated sum of the processes mentioned above. A numerical model can be used to partition the relative importance of those processes, but only with measurements in hand as validation. Therefore, confidently constraining the role of near-surface heat transfer processes requires temperature measurements with both high temporal and spatial resolution, and records that span hours to seasons.”

L13. 30 km below. . . is confusing. Rewrite. Also 1500m elevation in this area?

van de Wal et al. (2012) show the ELA fluctuating around 1500 m over the last 20 years. This was confusingly worded in our case though.

Changed sentence:

“The equilibrium line altitude is at about 1500 m elevation in this area (van de Wal et al., 2012), which is 400 m above the furthest inland site, 46-km, so all sites are well within the ablation zone and ablation rates are high (2-3 m/yr).”

L13: I miss info on elevation of the sites. Please add to Tab1

Added elevations.

L24: reduce numbers of sign digits

This is the number given on the datasheet for the sensor (DS18B20 from Maxim Integrated Products, Inc.)

L27: how was the field calibration done?

Changed to:

“field-calibrated with a temperature measurement during freeze-in (borehole water is exactly 0°C).”

L29: near surface: how near? Did you have a radiation shield? Add a picture of the AWS

Added:

“(~2-m) air temperature (Vaisala HMP60 with a radiation shield)”

Photo of the AWS was added to the supplement (Figure S2).

L34: how often were they re-aligned? Estimating from fig 3 there was a ca 6 m surface elevation change. This pushes your air temperature quite far into the near-surface inversion. How do you account for this.

Added: “with segments being removed from the mounting pole each summer so that the instrumentation stays close to the surface.”

P4 L4: why five strings?

We are trying to assess intra-site variability in near-surface ice temperature. This is how many strings were installed at site 33-km.

L11: how does that fit with field calibration P3 L27?

This was addressed in the comment above. The borehole water should be exactly 0°C.

L15: explain what positive and negative means for the gradients

Added “(positive being increasing temperature with depth below the surface)”

L15-17: unclear sentence. What do you mean?

Changed to:

“As expected, the temperature gradients measured here correlate well with the temperature gradients in the uppermost ~100 m for full-thickness temperature profiles measured at each site (Harrington et al., 2015; Hills et al., 2017).”

L21: makes things difficult. Consider only showing averages for concurrent times or at least full years? The rest does not make sense to me.

While we agree that the interpretation is more difficult for these sensor strings, we find it important to present all of the data. The three strings that failed in the springtime still provide valuable measurements especially below ~10 m where the seasonal variations are small.

For clarification we changed Figure 2 so that the failed strings are slightly transparent, and the caption is changed accordingly.

L26-27: this is a very large near-surface variability and not easy to understand. How about radiation errors of the uppermost sensors?

Added:

“Because each temperature sensor is in a black casing, measurements are discarded when the sensor lies on the surface exposed to the sun.”

L29: refer here to something you mark in the fig.

Figure 3 was significantly changed to point out the transient events.

P5 L5 see above. NOT net-shortwave

Deleted “shortwave”

L6: sounds low to me. Compare to Promice KAN stations? This could also help discriminating into SW and LW.

This was simply an error in the language. As was noticed, we repeatedly mentioned ‘shortwave’ radiation because of a previous draft of the manuscript, whereas we are now using net radiation. The numbers are more appropriate for mean daily net radiation.

L9: consider rewording ‘warm bias’

Changed to: “This warm anomaly between the ice and air temperature is also observed...”

L15-20: I believe that winter 2016 was particularly snow-poor and thus not particularly ‘representative’. Check if that is true on regional scale and include in discussion.

Looking at the data from PROMICE, KAN_L, it seems like this is in fact a representative snow year. 2015 was a much bigger snow year as can be seen in both our data and the PROMICE data.

Part 4 and 4.1. See issue with boundary condition (6). Boundary condition (7) is clearly not valid as you state yourself and adapt later. But why then introducing it and calling it a boundary condition? This does not make too much sense to me. The choice of experiments seems arbitrary. How about turbulent heat exchange?

Boundary condition (7) is altered as one of the experiments. For this reason, an insulating boundary (7) was used for the first 4 simulations with the specific intention of isolating the processes represented in each of those 4. When a heat flux is finally introduced in 4.2.4 we see the strong effect that it has on the near-surface temperature. It is in these contrasting model results that we see the significance of that bottom temperature gradient.

We consider only processes within the snow/ice (not the air above). Hence, the inversion and turbulent heat exchange are ignored.

P8 L9: net radiation

Deleted: “solar”

L25: $-0.05^{\circ}\text{C}/\text{m}$,

Deleted: “.”

P9 L5: also in other occasions surface temperature and air temperature can be very different

Added:

“Other atmospheric effects such as turbulent heat fluxes and the thermal inversion could also cause a difference between measured air temperature and ice surface temperature, but these are not considered here.”

L20: and

We are not sure what is being asked for here, but changed the sentence for clarity:

“Imposing a $-0.05^{\circ}\text{C}/\text{m}$ temperature gradient at the bottom of the model domain, consistent with observation, dramatically changes T_0 by -2.5°C .”

P10 2-4this seems trivial. If you keep the upper part of the ‘trumpet’ as it is and induce a gradient in 20m you will end up colder there. Is there a value in it?

We argue that our results show how important the subsurface temperature gradient is in controlling near-surface heat transfer and therefore melting in the ablation area. See P10 L26-33.

L24-25. What do you mean? Unique to the ablation zone. . .larger than other areas? Other ablation areas? The sentence does not make sense to me

Changed to:

“This conceptualization is unique to the ablation zone because of the rapid rate of surface lowering, whereas a diffusive model for near-surface heat transfer is much more appropriate for the accumulation zone.”

L30-34. Interesting. But what is the reason for such different ice-packages coming to the same site just a few dozens of m away? This should be better discussed and this high variability is potentially a significant result of the paper. How do satellite-derived surface temperatures vary spatially?

This process is discussed in detail in a previous paper that is referenced in the manuscript (Hills et al. 2017).

P11: L6. Refreezing is a big topic these days. Consider adding more refs Could the amount of water be estimated that would be necessary in order to reproduce the warming caused by latent heat you observe? This would be interesting.

Added:

“However, unlike firn, solid ice is impermeable to water unless fractures are present (Fountain et al., 2005).”

“In Greenland’s ablation zone, much work is being done to assess large-scale latent heating in open crevasses (Phillips et al., 2013; Poinar et al., 2016). Additionally, water-filled cavities have been observed in cold, near-surface ice on a mountain glacier (Jarvis and Clarke, 1974; Paterson and Savage, 1970). However, we are the first to show evidence of short-term transient latent heating events in cold ice.”

L26-29. Check out Colgan et al. Crevasse review. There is a process mentioned of crevasses ‘growing’ from below to the surface.

Added:

“Nath and Vaughan (2003) observed similar subsurface crevasses in firn, although in their case density was controlling the stiffness rather than temperature.”

P5-9: all that would point to ice being colder than air. But you show in fig 2 it is warmer. I doubt that the modelling serves as a base for this conclusion.

We added more analysis to the discussion to argue that the warm ice could be the result of two processes: the observed subsurface refreezing events, or a positive subsurface temperature gradient.

Fig 2 has a problem as it does not seem to account for changing surface height – I deduce this from the fact that each dot represents a sensor. It is, however, over time in different depths. Especially for the uppermost sensors this creates an issue. Suggest to correct the time-series using the known surface elevation changes. For the mean annual air temperatures. How do promice stations in the area fit to that? I am a bit worried about the height-above terrain and the radiation shield issue. Are air temperatures ventilated? Also: why don’t you sort them logically, i.e. from 27, 33 to 46? Add axes descriptions. Label a-g

We changed this figure so that temperatures are plotted at the time of measurement rather than the time of installation. We also added labels a-g and sorted based on time of installation.

We added a figure to the supplement which compares our AWS data to a nearby PROMICE station (Figure S4). Language was also added to the manuscript to address the radiation shield and height above surface:

“(Vaisala HMP60 with a radiation shield)”

“with segments being removed from the mounting pole each summer so that the instrumentation remains close enough to the surface that we are measuring ice surface conditions”

Figure 3: misleading. The depth of the sensor during installation is shown and not sensor depth. This is a massive difference. Strongly recommend to correct it for that. There are some interesting features and it is impossible to tell whether these are artefacts or reality. Which ones are the warming events you refer to? how about the vertical red lines, i.e. end of 2015 or ca may 2016 further down or again some time in spring 2017. Suggest indicating the

warming events you refer to later in the discussion. And what with the horizontal reddish bodies in late 2014 for instance in ca 8 m?

We made significant changes to many of the figures including Figure 3. We hope that we have addressed some of the confusion regarding identification of the events, as well as the other transient features in the dataset; namely, the freeze-in behavior (Figure 3b) which is now addressed in the manuscript as well.

Fig. 4: do they cool off again afterwards? Why don't you show the same time-steps in c and d as you do in a and b? how does meteorology play in here? Was there a rain-event preceding this? Impossible to tell if you don't state when it happened.

We feel that the way in which we have changed Figure 3 and the addition of the new Figure 7 help to illustrate when the refreezing events happen.

Fig. 5. b) consider combining b and c as surface elevation change D)If you measured with a NRLite p3, L30, you don't get net shortwave radiation to my understanding.

This figure was moved to the supplement.

We intentionally split (b) and (c) from the measured surface elevation change so that the steps of the modeling exercise are more clear.

Deleted: "shortwave"

Processes influencing ~~near-surface~~ heat transfer in the ~~near-surface~~ ice of Greenland's ablation zone

Benjamin H. Hills^{1,2}, Joel T. Harper², Toby W. Meierbach¹, Jesse V. Johnson³, Neil F. Humphrey⁴, Patrick J. Wright^{5,2}

¹Department of Earth and Space Sciences, University of Washington, Seattle, Washington, USA

²Department of Geosciences, University of Montana, Missoula, Montana, USA

³Department of Computer Science, University of Montana, Missoula, Montana, USA

⁴Department of Geology and Geophysics, University of Wyoming, Laramie, Wyoming, USA

⁵Inversion Labs LLC, Wilson, Wyoming, USA

Correspondence to: Benjamin H. Hills (bhills@uw.edu)

Abstract. To assess the influence of various ~~mechanisms of~~ heat transfer mechanisms on the temperature structure of ice near ~~the~~ ice of Greenland's ablation zone, we ~~incorporate compare~~ highly resolved in situ measurements ~~of ice temperature into with simplified~~ thermal modeling experiments. Seven separate temperature strings were installed at three different field sites, each with between 17 and 32 sensors and extending up to 2120 meters below the surface. In one string, temperatures were measured every 30 minutes, and the record is continuous for more than three years. We use these measured ice temperatures to constrain modeling analyses focused on four isolated processes ~~and to~~ assess the relative importance of each ~~for to~~ the near-surface ice temperature: 1) the moving boundary of an ablating surface, 2) thermal insulation by snow, 3) radiative energy input, and 4) subsurface deep ice temperature gradients below the seasonally active near-surface layer. In addition to these four processes, transient heating events were observed in two of the temperature strings. Despite no observations of meltwater pathways to the subsurface, these heating events are likely the refreezing of liquid water below 5-10 meters of cold ice. Together with subsurface refreezing, the five heat transfer mechanisms presented here account for measured differences of up to 3°C between the mean annual air temperature and the ice temperature at the depth where annual temperature variability is dissipated and the mean annual air temperature. Thus, in Greenland's ablation zone, the mean annual air temperature ~~cannot be used to is not a reliable~~ predictor of the near-surface ice temperature, as is commonly assumed.

1 Introduction

Ice sheets are coupled to the atmosphere at their upper surface through an exchange of mass and energy. Understanding this coupling is important for knowing the ice sheet's surface mass balance and its associated contribution to sea level rise. In particular, the Greenland Ice Sheet (GrIS) has shown a change toward a more negative surface mass balance, which constitutes at least half of its contribution to recent sea level rise (van den Broeke et al., 2009; Enderlin et al., 2014). In Bare ice high melt regions of the Greenland ice sheet have high summer melt rates. Here, the surface ice temperature is important to ablation processes such as melt, water storage, runoff, and albedo modifications associated with the surface cryoconite layer (Wharton et al., 1985). The ice surface temperature also acts as an essential boundary condition for the transfer of heat into deeper ice below, and is therefore important for ice flow modeling (e.g. Meierbachtol et al., 2015) as well as interpretation of borehole temperature measurements (Harrington et al., 2015; Hills et al., 2017; M.P. Lüthi et al., 2015). In order to constrain the rate of ice melting, and more generally to understand the mechanisms which move energy between the ice and the atmosphere above climate systems, we must understand the processes that control near-surface heat transfer in bare ice.

Heat transfer at the ice surface is dominated by thermal diffusion from the overlying air (Cuffey and Paterson, 2010). Seasonal air temperature oscillations are diminished with depth into the ice, until they are negligible (i.e. ~1%) at a 'depth of zero annual amplitude' (van Everdingen, 1998). The exact location of this depth is dependent on the thermal diffusivity of the material through which heat is conducted as well as the period of oscillations (Carslaw and Jaeger, 1959; pp. 64-70). In theory, the temperature at the depth of zero annual amplitude, a value we will call T_0 , is approximately constant and equal to the mean annual air temperature. In snow and ice, the depth of zero annual amplitude is approximately 10 and 15 m respectively (Hooke, 1976). For this reason, studies in the cryosphere often use T_0 as a proxy for the mean air temperature, drilling to 10 or more meters to measure the snow or ice temperature at that depth (Loewe, 1970; Mock and Weeks, 1966).

In places where heat transfer is purely diffusive, the snow or ice is homogeneous, and interannual the climate variations are minimal, forcing is constant, T_0 is a good approximation for the mean air temperature. However, prior studies have shown that, in many areas of glaciers and ice sheets, the relationship between air and ice temperatures can be substantially altered by additional heat transfer processes. For example, in the percolation zone, infiltration and refreezing of surface meltwater warm the subsurface (Humphrey et al., 2012; Müller, 1976). Studies have also revealed ice anomalously warmed by 5°C or more in the ablation zone (Hooke et al., 1983; Meierbachtol et al., 2015), but the mechanisms for this are unclear.

Hooke et al. (1983) explored the impacts of several heat transfer processes within near-surface ice at Storglaciären and the Barnes Ice Cap. They focused on the wintertime snowpack which acts as insulation to cold air temperatures but is permeable to meltwater percolation. Their results showed that the average ice temperature at and below the equilibrium line of those glaciers tends to be higher than the mean annual air temperature. They attributed the observed difference mainly to snow insulation because the strength of their measured offset was correlated to the thickness of the snowpack.

In this study, we expand the analysis of Hooke et al. (1983) and turn focus to the GrIS ablation zone with near-

surface temperature profiles from seven locations. We ~~use use those~~our temperature measurements in conjunction with a one-dimensional heat transfer model to assess heat transfer processes in this area. The processes which make the ablation zone different from other areas of ~~the GrIS area glacier or ice sheet are~~, first, that the ice surface spends much of the summer period pinned at the melting point, despite slightly ~~warmer~~~~higher~~ air temperatures. Next, high ablation rates counter emerging ice flow, removing the ice surface and exposing deeper ice, along with its heat content, to the surface. ~~Further, he contrast of a wintertime snowpack to bare ice in the summer enables an insulating effect during the winter months~~~~the ice from cold winter temperatures~~~~T~~, and the absorption deep penetration of solar radiation ~~into bare ice~~ results in ~~subsurface~~ heating and melting (R. Brandt ~~and~~ Warren, 1993; Liston et al., 1999)~~of ice~~. Finally, surface melt can move through open fractures, carrying latent heat with it to deeper and colder ice, and upon refreezing, the meltwater warms that ice below the surface (Jarvis ~~and~~ Clarke, 1974; Phillips et al., 2010).

Our

~~Each of these processes can be simulated numerically. near-surface temperature observations represent an aggregated sum of the processes mentioned above. A numerical model can be used to partition the relative importance of those processes, but only with measurements in hand as validation. Therefore, However, a quantitative comparison of the competing processes can only be derived through observation. C~~onfidently constraining the role of ~~near-surface heat transfer each of these~~ processes requires ~~in-situ~~ temperature measurements with both high ~~time-temporal~~ and ~~spatial~~ resolution, and records that span hours to seasons.

2 Field Site and Instrumentation

Field observations used in this study are from three sites in western Greenland (Figure 1). Each site is named by its location with respect to the terminus of Isunnguata Sermia, a land-terminating outlet glacier. ~~The equilibrium line altitude is at about 1500 m elevation in this area~~ (van de Wal et al., 2012), ~~which is 400 m above the~~ ~~The~~ furthest inland site, 46-km, ~~is ~30 km below the equilibrium line altitude which is at about 1500 m elevation~~ [van de Wal et al., 2012], so all sites are well within the ablation zone and ablation rates are high (2-3 m/yr). Solar radiation in the summer creates a layer of interconnected cryoconite holes at the ice surface, and water moving through that cryoconite layer converges into surface streams. There are no large supraglacial lakes in the immediate area of any site; all streams eventually drain from the surface through moulins. A series of dark folded layers emerge to the ice surface in this region of the ice sheet (Wientjes ~~and~~ Oerlemans, 2010).

At each field site, boreholes for temperature instrumentation were drilled from the surface to ~~between -120 and 21~~ m depth using hot-water methods. In total, seven strings of temperature sensors were installed – one at both sites 27-km and 46-km in 2011, followed by five at site 33-km between 2014 and 2016. Strings are named by the year they were installed. Each consists of between 17 and 32 sensors spaced at 0.5-3.0 m along the cable (Table 1). In 2011 and 2014, thermistors were used as temperature sensors. The thermistors have measurement resolution of 0.02°C and accuracy of about 0.5°C after accounting for drift (Humphrey et al., 2012). In subsequent years, we used a digital temperature sensor (model DS18B20 from Maxim Integrated Products, Inc.). This sensor has resolution 0.0625°C and about the same accuracy as the thermistors. To increase accuracy, each sensor was lab-calibrated in a

0°C bath, and field-calibrated [with a temperature measurement](#) during [borehole](#) freeze-in ([borehole water is exactly 0°C](#)). [Because each temperature sensor is in a black casing, measurements are discarded when the sensor lies on the surface exposed to the sun.](#)

Meteorological variables were measured at each field site as well, [using standard Campbell Scientific products](#). In this study, we use the near-surface ([~2-m](#)) air temperature (Vaisala HMP60 [with a radiation shield](#)), the net radiative heat flux over all wavelengths shorter than 100 μm (Kipp and Zonen NR Lite), and the change in surface elevation measured with a sonic [ranger-distance sensor](#) (Campbell SR50A). [Data from the sonic distance sensor are filtered manually, removing any obvious outliers \(more than 0.5 m from the surrounding measurements\). The filtered data are then partitioned into](#) ~~two variables are taken from the sonic ranger~~, cumulative ablation during the melt season and changes in snow depth during the winter. An automated weather station with all the above instrumentation was mounted on a fixed pole frozen in the ice, [with segments being removed from the mounting pole each summer so the instrumentation remains close to the surface and does not extend significantly into the air temperature inversion](#) (Miller et al., 2013). ~~The~~ The measurement frequency for meteorological data varies from ten minutes to an hour, but all data are collapsed to a daily mean for input to a heat transfer model.

In addition to ice temperature and meteorological measurements, investigations of the subsurface were completed at site 33-km with a borehole video camera, and [with](#) a high-frequency ground-penetrating radar survey ([see](#) [supplementary](#)). These investigations were carried out in pursuit of what we think may have been subsurface fractures that are not expressed at the ice surface (described in section 5.2). With five temperature sensor strings, an automated weather station station, and the subsurface investigations, site 33-km is by far the most thoroughly studied of the three sites. For that reason, measurements from this site serve as the foundation for [the](#) model case study presented in section 4.

3 Results

3.1 Observed Ice Temperature

Near-surface ice temperatures were measured through time in seven shallow boreholes at three different field sites (Figure 2). Although hot-water drilling methods temporarily warm ice near the instrumentation, the ice around these shallow boreholes cools to its original temperature within days to weeks. ~~M~~The measured temperatures are spatially variable between sites, [with a. The mean value from the lowermost sensor- \(analogous to \$T_0\$ \) is](#) -3.2 at 27-km, -8.6 at 46-km, and from -9.7°C to -8.1 at 33-km. In all cases, measured T_0 values are warmer than the mean annual air temperature. Temperature gradients [are calculated by fitting a line to the mean temperature of the four lowermost sensors for each string, at 20 m](#) [These gradients](#) are also variable, [typically](#) [typically](#) being between -0.15 and 0.00°C/m but +0.16°C/m at the 27-km field site ([positive](#) being increasing temperature with depth below the surface). [As expected, As expected, the](#) direction of [variability in the](#) temperature gradients [at the bottom of the profiles](#) measured here correlate with those measured [in the uppermost ~100 m](#) [observations offor](#) full-thickness [deeper](#) temperature profiles [measured at each site](#) (Harrington et al., 2015; Hills et al., 2017).

Even the five temperature profiles measured at site 33-km exhibit some amount of spatial variability. Three

temperature strings, T-15a, b, and c, are all similar, having strong negative temperature gradients (approximately ranging from -0.1 to $-0.045^{\circ}\text{C}/\text{m}$), and cold T_0 temperatures (approximately -9.65°C). Close to the surface, these three temperature strings appear to be rather cold compared to the others. However, those strings stopped collecting measurements failed in May 2017 and did not yield a full year of data. The missing summer period explains the mean cold bias strong positive temperature gradient near the surface for those three strings. T-16 is the shortest string, only string that did not reach 20 m. This short string extended to only 9.5 m depth. This short string exhibits the and measured the smallest range in temperatures throughout a season with the coldest surface temperatures not even reaching -15°C . In terms of mean temperature, T-16 is similar to T-14, having a small negative temperature gradient and warm temperatures in comparison to those of T-15. Based on our these observations, spatial variability in near-surface ice temperature at site 33-km is controlled on the scale of hundreds of meters. Proximal observations from the three nearby T-15 strings are similar to one another, but greater variability is observed when including the more distant strings, T-14 and T-16.

Closer inspection of the measured temperature record through time reveals the transient nature of near-surface ice temperature (Figure 3). As expected, these data show a strong seasonal oscillation near the surface. During the melt season, the ice surface quickly drops after near surface as ice is warmed to the melting point. Just below the surface, the winter cold wave persists for several weeks into the summer season. For this particular string, T-14, delayed freeze-in behavior was observed in one sensor (Figure 3b) and transient heating events were observed during the melt seasons (Figure 3c, 3d, 3e). Similar heating events were observed in the T-16 string (Figure 4), but not in any other. The events range in magnitude, but in one instance ice is warmed from -10°C to -2°C in 2 hours (Figure 3c). We can only speculate on the origins of these events, and address this below in section 5.2.

3.2 Meteorological Data

Meteorological data from site 33-km were observed over three years (supplementary Figure S4)-(Figure 5). Air temperatures are normally at or above the melting temperature during the summer but fall to below -30°C in winter months. The measured ablation rate is on the order of 2-3 m/yr and maximum snow accumulation is only up to 0.5 m. Net shortwave radiation is less than zero in the winter (net outgoing because of thermal emission in the infrared wavelengths) but over 100 W/m^2 (daily mean) on some days in the summer.

The mean air temperature over the entire measurement period at site 33-km (-10.5°C) is cold in comparison to measured ice temperatures at that site (Figure 2; T-14, T-15, and T-16). This warm anomaly between the ice and air temperature bias in the near-surface ice temperature is also observed at sites 27-km and 46-km, where ice is warmer than the measured air temperature and significantly warmer than the reference from a regional climate model (Meierbachtol et al., 2015). Interestingly, we measure almost no winter snowpack at sites 27-km and 46-km due to low precipitation and strong winds during the time period over which those data were collected (2011-2013). Our observations are thus in contradiction to the inferences made by Hooke et al. (1983) in Arctic Canada, where who said that the offset between air and ice temperature appeared to be is primarily a result of snow insulation. Overall, the three years for which meteorological data were collected are significantly different. The 2014-15 winter was particularly cold, bringing the mean air temperature of that year more than a degree lower than the other two

seasons. Snow accumulation was approximately doubled that winter in comparison to the other two. Also, the summer melt season is longer in 2016 than in 2015. In comparison with past trends from a nearby site, [KAN LIMAUS6](#), the second year is more typical for this area (van As et al., 2012). To model a representative season, data from that second year (July 2015 to July 2016) were chosen as annual input for the model case study.

4 Analysis

Our objective is now to investigate how various processes active in Greenland's ablation zone influence T_0 . In order for model results to achieve fidelity, inputs and parameters need to be representative of actual conditions. We therefore use the [observational-meteorological data](#) to constrain the modeling experiments. Our modeling is focused at field site 33-km, where we have the most data for constraining the problem.

4.1 Model Formulation

The foundation for quantifying impacts of near-surface heat-transfer processes is a one-dimensional thermodynamic model. [We argue that the processes tested here are close enough to being homogeneous that they can be adequately assessed in one dimension. The one exception is the measured heating events which are transient and spatially discrete, these are discussed in section 5.2 and are not included in the model analysis.](#) Our model uses measured meteorological variables as the surface boundary condition and simulates ice temperature to 210 m, a depth chosen for consistency with measured data. The ice temperature at the depth of zero annual amplitude, T_0 , is output from the bottom of the domain for each model experiment and used as a metric to compare net temperature changes between simulations. [The model, its boundary conditions, and the experiments are all designed to test heat transfer processes within the ice itself. To maintain focus on ice processes, we ignore any atmospheric effects above the ice surface such as turbulent heat fluxes.](#) The model does not, nor is it meant to, simulate the surface mass balance.

We implement an Eulerian framework, treating the z dimension as depth from a moving surface boundary so that emerging ice is moving through the domain and is removed when it melts at $z = 0$. We use a finite element model with a first-order linear element [and 0.5-m mesh spacing refined to 2 cm near the surface](#). For a seamless representation of energy across the water/ice phase boundary, we implement an advection-diffusion enthalpy formulation (i.e. Aschwanden et al., 2012; Brinkerhoff and Johnson, 2013),

$$(\partial_t + w\partial_z)H = \partial_z(\alpha\partial_z H) + \phi/\rho_i \quad (1)$$

Here, ∂ is a partial derivative, t is time, w is the vertical ice velocity with respect to the lowering ice surface, z is depth, H is specific enthalpy, α is diffusivity, ϕ is any added energy source, and ρ_i is the density of ice. The diffusivity term is enthalpy-dependent,

$$\alpha(H) = \begin{cases} k_i/\rho_i C_p & \text{cold, } H < H_m \\ v/\rho_i & \text{temperate, } H > H_m \end{cases} \quad (2)$$

where k_i is the thermal conductivity of ice which we assume is constant over the small temperature range in this

study ($\sim 25^\circ\text{C}$), C_p is the specific heat capacity which is again assumed constant, ν is the moisture diffusivity in temperate ice, and H_m is the reference enthalpy at the melting point (all constants are shown in Table 2).

Aschwanden et al. (2012) include a thermally diffusive component in temperate ice (i.e. $k_i \partial_z^2 T_m(P)$). However, since we consider only near-surface ice, where pressures (P) are low, this term reduces to zero. Using this formulation, energy moves by a sensible heat flux in cold ice and a latent heat flux in temperate ice. We assume that the latent heat flux, prescribed by a temperate ice diffusivity (ν/ρ_i), is an order of magnitude smaller than the cold ice diffusivity ($k_i/\rho_i C_p$). We argue that this is representative of the near-surface ice when cold ice is impermeable to meltwater.

The desired model output is ice temperature. It has been argued that temperature is related to enthalpy through a continuous function, where the transition between cold and temperate ice is smooth over some ‘cold-temperate transition surface’ (M. Lüthi et al., 2002). On the other hand, we argue that cold ice is completely impermeable to water except in open fractures (which we do not include in these simulations), so we use a stepwise transition,

$$T(H) = \begin{cases} (H - H_m)/C_p + T_m & \text{cold} \\ T_m & \text{temperate} \end{cases} \quad (3)$$

Additional enthalpy above the reference increases the water content in ice,

$$\omega(H) = \begin{cases} 0 & \text{cold} \\ (H - H_m)/L_f & \text{temperate} \end{cases} \quad (4)$$

where L_f is the latent heat of fusion. If enough energy is added to ice that its temperature would exceed the melting point, excess energy goes to melting. In our case study, we limit the water content based on field observations of water accumulation in the layer of rotten ice and cryoconite holes. This rotten cryoconite layer extends to approximately 20 cm deep and as an upper limit accumulates a maximum 50% liquid water. Therefore, we limit the water content in the rotten cryoconite layer,

$$0.0 \leq \omega \leq 0.5 \quad (5)$$

with any excess water immediately leaving the model domain as surface runoff.

The two boundary conditions are 1) fixed to the air temperature at the surface,

$$T(\text{surface}, t) = T_{\text{air}} \quad (6)$$

and 2) free at the bottom of the domain,

$$\frac{\partial T}{\partial z_{\text{bottom}}} = 0.0 \quad (7)$$

Both boundary conditions are with no liquid water content, $\omega = 0$. The surface boundary condition is updated at each time step to match the measured air temperature. The bottom boundary condition is fixed in time. This bottom boundary condition is also changed for some model experiments to test the influence of a temperature gradient at the

bottom of the domain (section 4.2.4).

4.2 Experiments

Four separate model experiments are run, each with a new process incorporated into the [model](#) physics, and [each](#) guided by observational data. All simulations use the enthalpy formulation above rather than temperature in order to track the internal energy of the ice/water mixtures that are prevalent in the ablation zone. Each experiment is referenced to an initial control run which reflects simple thermal diffusion of the measured air temperature in the absence of any additional heat transfer processes. Meteorological data are input where needed for an associated process in the model. These data are clipped to one full year and input at the surface boundary in an annual cycle. The model is run with a one-day time step until ice temperature at the bottom of the domain converges to a steady temperature. A description of each of the model experiments follows below. These experiments build on one another, so each new experiment incorporates the physics of all previously discussed processes.

4.2.1 Ablation

The first experiment simulates motion of the ablating surface. While the control run is performed with no advective transport (i.e. $w = 0$), in this experiment we incorporate advection by setting the vertical velocity equal to measurements of the changing surface elevation through time. When ice melts the ice surface location drops. Because the vertical coordinate, z , in the model domain is treated as a distance from the moving surface, ablation brings simulated ice closer to the surface boundary. Hence, the simulated ice velocity \underline{w}_z is assigned to the ablation rate (except in the opposite direction, ice moves upward) for this first model experiment. The ablation rate is calculated as a forward difference of the measured surface lowering.

4.2.2 Snow Insulation

The second experiment incorporates measured snow accumulation, which thermally insulates the ice from the air. The upper boundary condition is assigned to the snow surface, whose location changes in time. Diffusion through the snowpack is then simulated as an extension of the ice domain but with different physical properties. The thermal conductivity of snow (Calonne et al., 2011),

$$k_s = 2.5 * 10^{-6} \rho_s^2 - 1.23 * 10^{-4} \rho_s + 0.024 \quad (8)$$

is dependent on snow density, ρ_s , for which we use a constant value, 300 kg/m^3 . We treat the specific heat capacity of snow to be the same as ice (Yen, 1981).

4.2.3 Radiative Energy

The third model experiment incorporates an energy source from the net [solar](#) radiation measured at the surface. Energy from radiation is absorbed in the ice and is transferred to thermal energy and to ice melting (van den Broeke et al., 2008). We assume that all this radiative energy is absorbed in the uppermost 20 cm, the rotten cryoconite layer, and if snow is present the melt production immediately drains to that cryoconite layer. When the net radiation

is negative (wintertime) we assume that it is controlling the air temperature, so it is already accommodated in our simulation; thus, the radiative energy input is ignored in the negative case. This radiative source term, is incorporated into equation (1) at each time step $\phi_{rad} = \frac{Q}{20cm}$, where Q is the measured radiative flux at the surface in W/m^2 . All constants for the rotten cryoconite layer are the same as that for ice.

While some models treat the absorption of radiation in snow/ice more explicitly with a spectrally-dependent Beer-Lambert Law (Brandt and Warren, 1993), we argue that it is reasonable to assume that all wavelengths are absorbed near the surface over the length scales that we consider. The only documented value that we know of for an absorption coefficient in the cryoconite layer is 28 m^{-1} (Lliboutry, 1965) which is close to that of snow (Perovich, 2007). If the properties are truly similar to that of snow, about 90 percent of the energy is absorbed in the uppermost 20 cm (Warren, 1982). Moreover, we argue that this is precisely the reason that the cryoconite layer only extends to a limited depth; it is a result of where radiative energy causes melting.

4.2.4 Subsurface 20 m Temperature Gradient

Finally, in the fourth model experiment we change the boundary condition at the bottom of the domain. The free boundary is changed to a Neumann boundary with a gradient of -0.05°C/m , a value that approximately matches the measured gradient in our near-surface temperature measurements at site 33-km at field site 33-km. Importantly, this simulated gradient is in the same direction, although with a larger magnitude, of the upper $\sim 100 \text{ m}$ of ice in our measurements of deep temperature profiles (Hills et al., 2017). In this case, the advective energy flux is upward, but the temperature gradient is negative, bringing colder ice to the surface. In addition, two limiting cases were tested, with gradients of $\pm 0.15^\circ\text{C/m}$. This is the approximate range in measured gradients (Figure 2).

4.3 Model Results

The control model run of simple thermal diffusion predicts that ice temperature damps to approximately the mean annual air temperature of the study year (-9.9°C) by about 15 m below the ice surface. This result is in agreement with the analytical solution (Carslaw and Jaeger, 1959), but slightly different from the mean air temperature (-9.6°C) because the air can exceed the melting temperature in the summer while the ice cannot. Other atmospheric effects such as turbulent heat fluxes and the thermal inversion could also cause a difference between measured air temperature and ice surface temperature, but these are not considered here. For each model treatment, 1-4, the incorporation of an additional physical process changes the ice temperature. Differences between model runs are compared using T_0 at 2¹⁰ m. Again, the model experiments are progressive, so each new experiment includes the processes from all previous experiments. Key results from each experiment are as follows (Figure 56):

1. Diffusion alone results in $T_0 = -9.9^\circ\text{C}$, whereas observed temperatures range from -9.7°C to -8.1 at the 33-km field site.
2. Because the ablation rate is strongest in the summer, the effect of incorporating ablation is to counteract the diffusion of warm summer air temperatures. The result is a net cooling of T_0 from experiment (1) by -0.92°C .

3. Snow on the ice surface insulates the ice from the air temperature. In the winter, snow insulation keeps the ice warmer than the cold air, but with warm air temperatures in the spring it has the opposite effect. Because snow quickly melts in the springtime, the net effect of snow insulation is substantially more warming than cooling. T_0 for this experiment is $+0.78^\circ\text{C}$ warmer than the previous.
4. Radiative energy input mainly controls melting (van den Broeke et al., 2008), but incorporating this process does warm T_0 by $+0.52^\circ\text{C}$.
5. Imposing a $-0.05^\circ\text{C}/\text{m}$ temperature gradient at the bottom of the model domain, consistent with observation, dramatically changes T_0 by -2.5°C .

Both ablation and the subsurface temperature gradient have a cooling effect on near-surface ice temperature. On the other hand, snow and radiative energy input have a warming effect. For this case study, the first three processes together result in almost no net change so that the modeled T_0 is close to the observed mean air temperature (Figure 56d). However, inclusion of the subsurface temperature gradient has a strong cooling effect on the simulated temperatures, bringing T_0 far from the mean measured air temperature. The limiting cases show that this bottom boundary condition strongly controls the near-surface temperature, with a range in the resulting T_0 values from -17.0°C to -2.0°C . In summary, measured ice temperatures are consistently warmer than both the measured air temperature and simulated ice temperature (Figure 67), except in the case of a positive subsurface gradient which is discussed below.

5 Discussion

Our observations show that measurements of near-surface ice in the ablation zone of western Greenland are significantly warmer than would be predicted by diffusive heat exchange with the atmosphere. This is in agreement with past observations collected in other ablation zones (e.g. Hooke et al., 1983). With four experiments in a numerical model that progressively incorporate more physical complexity, we are unable to precisely match independent model output to observations. Our measurement and model output consistently point toward a disconnect between air and ice temperatures in the GrIS ablation zone, with ice temperatures being consistently warmer than the air.

5.1 Ablation-Diffusion

The strongest result from our model case study was a drop in T_0 by -2.5°C associated with the imposed subsurface deep ice negative 20 m temperature gradient. While it was important to test this scenario for one case, the temperature gradient we used was representative, but somewhat arbitrary. In reality, the observed 20 m temperature gradients is are widely variable from one site to another and even within one site (Figure 2). Interestingly, full ice thickness temperature profiles show similar temperature gradients, both positive and negative, that persist for many hundreds of meters toward the bed (Harrington et al., 2015; Hills et al., 2017). Hence, the limiting cases were added to show simulation results over the range of measured gradients from our temperature strings. The resulting T_0 span a range of 19°C .

Our model could have tested additional temperature gradients, and those of the opposite (positive) sign likely would

have fit our measured T_0 much better. However, we argue that this would have been a simple model tuning exercise to match data, whereas our purpose is to elucidate the relationship between near-surface ice temperature and ablation/emergence. The majority of the subsurface Furthermore, the deep ice temperature gradients that we measure are negative, and theoretically the gradient should be negative should theoretically be negative in the ablation zone.

Consider that fast horizontal velocities (~ 100 m/yr) advect cold ice from the divide to the ablation zone, and the air temperature lapse rate couples with the relatively steep surface gradients so that the surface warms rapidly toward the terminus. These conditions lead to a vertical temperature gradient below the ice surface that is negative (Hooke, 2005; pp. 131-135), as in our model example. The one exception is in the case of deep latent heating in a crevasse field (Harrington et al., 2015; sites S3 and S4) where the deep ice temperature would be warmer than the mean air temperature rather than colder.

Importantly, our Overall, our results demonstrate that the effect of the subsurface 20 m temperature gradient is coupled to that of surface lowering. With respect to the surface, the temperature gradient below is advected upward as ice melts. There is a competition between surface lowering and diffusion of atmospheric energy into the ice; as near-surface ice is warmed, it can be removed quickly and a new boundary set. Therefore, our conceptualization of temperature in the near-surface ice of the ablation zone should not be a seasonally oscillating upper boundary with purely diffusive heat transfer (Carslaw and Jaeger, 1959), but one with advection and diffusion (Logan and & Zlotnik, 1995; Paterson, 1972). This conceptualization is unique to the ablation zone because of the its high ablation rates rapid rate of surface lowering, which are at least an order of magnitude larger than other areas whereas a diffusive model for near-surface heat transfer is much more appropriate in the accumulation zone.

The implications for the The disconnect between air and ice temperature implies that are that the near-surface active layer in the ablation zone is shallow small (i.e. less than 15 m) and could be skewed toward the subsurface 20 m temperature gradient. Therefore, the surface boundary condition has a much weaker influence on diffusion for ice well below the surface. This is in contrast to the accumulation zone where new snow is advected downward, so the surface temperature quickly influences that at depth than it would in other areas of the ice sheet. Additionally, melting dynamics are complicated by the 20 m temperature gradient. Under these conditions, it is no surprise that we see spatial variability in near-surface ice temperature even within one field site. That variability is simply an expression of the deeper ice temperature variations which are hypothesized to exist from variations in vertical advection (Hills et al., 2017), and do not have time to completely diffuse away before they are exposed at the surface.

5.2 Subsurface Refreezing

In two temperature strings we observe transient heating events, the largest case being as much as 8°C in 2 hours between 3 and 8 m below the ice surface (Figure 3c). We argue that the most likely energy source for such events is latent heat because the These events are transient, they are spatially discrete, and they are generated at from depth, all of which are most easily explained by. This implies that the heating observations are due to the refreezing of liquid water in cold ice. Similar refreezing events have been observed in firn (Humphrey et al., 2012), where they are not only important for ice temperature but could also imply a large storage reservoir for surface meltwater (Harper et al.,

2012). However, unlike firn, solid ice is impermeable to water unless fractures are present (Fountain et al., 2005).

In Greenland's ablation zone, much work is being done to prior work has demonstrated the importance of assess large-scale latent heating in open crevasses (Phillips et al., 2013; Poinar et al., 2016). Additionally, while water-filled cavities have been observed in cold, near-surface ice on at least one a mountain glaciers (Jarvis and Clarke, 1974; Paterson and Savage, 1970). In our case, however, a mechanism for sudden water movement to depth is an explanation for refreezing water is not obvious: while the field site has occasional mm-aperture 'hairline' cracks, there are but no visible open crevasses at the surface for routing water to depth.

However, As far as we know, this work is we are the first to report show evidence of short-term transient latent heating events in cold ice, not obviously linked to open surface fractures.

While the hairline and Fountain et al. (2005) suggest that fractures provide the main pathway for liquid water to move through temperate ice, a mechanism for sudden water movement to depth in the ablation zone of Greenland is not obvious. Fractures could perhaps move some are the most likely pathway to move water to depth, but to permit move much water to move meters through cold ice they would need to be large enough that water moves quickly, and does not instantaneously refreeze. For example, A a 1-mm wide crack in ice that is -10°C freezes shut in about 45 seconds (Alley et al., 2005; eq. 8). Assuming that there is a hydraulic potential gradient to drive water flow, that amount of time could be long enough for small volumes of water to move at least 5-10 m below the surface, but would require a hydropotential gradient to drive water flow through cold ice. Thus, top-down hairline crevassing does not seem a plausible explanation for the events we observe.

A mechanism for sudden water movement to depth at our field site, 33 km, is not obvious. The field site at 33 km has no visible open crevasses at the surface, but does have occasional mm-aperture cracks.

Nevertheless, Importantly, several independent field observations in this area including hole drainage of water during hot-water drilling, ground-penetrating radar reflections, and borehole video observations, all pointing to the existence of subsurface air-filled and open fractures with apertures of up to a few cm (see supplementary). We suggest that these features occasionally move water to ~10 m below the ice surface, where it refreezes and warms the ice as we have observed. That they are open at depth, but are narrow or non-existent at the surface, could be linked to the colder ice at depth and its stiffer rheology. Nath and Vaughan (2003) observed similar subsurface crevasses in firn, although in their case density controls the stiffness rather than temperature. We suggest that these features occasionally move water to ~10 m below the ice surface, where it refreezes and warms the ice as we have observed.

On rare occasions, we argue that the aperture of the fractures open wider to the surface, where there is copious water stored in the cryoconite layer (Cooper et al., 2018) that can drain and refreeze at depth (Cooper et al., 2018). While

the events seem to happen in the springtime and it would be tempting to assert that fracture opening coincides with speedup, our measurements of surface velocity at these sites show that this is not always the case. This may be due to that fact that the spring speed up coincides with early melt rather than peak melt and copious water in the cryoconite layer.

Latent heating in the form of these subsurface refreezing events is an obvious candidate for the source of the ‘extra’ heat that we observe in our temperature strings relative to simulations. Our data show that refreezing in subsurface fractures has the potential to warm ice substantially over short periods of time, and apparently this can occur in places where crevasses are not readily observed at the surface. Furthermore, the difference between measured and modeled temperatures ($\sim 3^\circ\text{C}$) is the equivalent of only $\sim 1.7\%$ water by volume. Our simplified one-dimensional model would not be well-suited to assess the influence of these latent heating events. Instead, we provide a simple calculation for energy input from the events by differencing the temperature profiles in time and integrating for total energy density (Figure 7 a-c).

$$\phi_{measured} = \frac{\rho_i C_p}{\Delta z} \int \Delta T \, dz \quad (9)$$

where Δz is the total depth of the profile, and ΔT is the differenced temperature profile. Only sensors that are below the ice surface for the entire time period are considered. To calculate the total water content refrozen in the associated event, we remove the conductive energy fluxes from the total energy density calculated above. We do so by calculating the temperature gradients at the top and bottom of the measured temperature profile at each time step as in Cox et al. (Cox et al., 2015).

$$\phi_{conductive} = \frac{-k_i}{\Delta z} \int \frac{\partial T}{\partial z}_{top} - \frac{\partial T}{\partial z}_{bottom} \, dt \quad (10)$$

The resulting energy sources are then converted to a volume fraction of water by

$$\omega_{measured} = \frac{\phi_{measured} - \phi_{conductive}}{\rho_w L_f} \quad (11)$$

where ρ_w is the density of water. Results show that each year some fractions of a percent of water are refrozen (Figure 7 d-f). Through several seasons that amount of refreezing could easily add up to the $\sim 3^\circ\text{C}$ anomaly that we observe.

Latent heating is an obvious candidate for the source of ‘extra’ heat that we observe in our temperature strings relative to simulations. Our data show that refreezing in subsurface fractures has the potential to warm ice substantially over short periods of time, and apparently this can occur in places where crevasses are not readily observed at the surface. However, unfortunately, without a more thorough investigation, we have not had enough evidence to show that these refreezing events are more than a local anomaly. Of our seven near-surface temperature strings, only T-14 and T-16 demonstrated refreezing events, and so we are not confident that they are temporally or spatially ubiquitous.

The only other logical ~~mechanisms~~ for the warm ~~offset between measurements and model results~~ would ~~be warming from below through a positive subsurface temperature gradient~~.

While it is tempting to associate deep warm ice with ~~either residual heat from the exceptionally hot summers of a strong warm event in previous years such as in 2010 and 2012~~ (Tedesco et al., 2013), ~~this scenario is unlikely because the ablation rates are so high that any ice warmed during those years has likely already melted. Deeper latent heating from an upstream crevasse field is a more plausible alternative~~(van As et al., 2012), ~~or possibly deeper latent heating from an upstream crevasse field. In those cases, a positive 20 m deep temperature gradient would promote warming near the surface~~; however, in this area full-depth temperature profiles do not show deeper ice to be anomalously warmed except in one localized case (Hills et al., 2017).

6 Conclusion

We observe the temperature of ice at the depth of zero annual amplitude, T_0 , in Greenland's ablation zone to be markedly warmer than the mean annual air temperature. These findings contradict predictions from purely diffusive heat transport but are not surprising considering the processes which impact heat transfer in ice of the ablation zone. High ablation rates in this area indicate that ice temperatures below ~15 m reflect the temperature of deep ice that is emerging to the surface, confirming that the ice does not have time to equilibrate with the atmosphere. In other words, ice flow brings cold ice to the surface at a faster rate than heat from the atmosphere can diffuse into the ablating surface. The coupling between rapid ablation and the spatial variability in deep ice temperature implies there will always be a disconnect between air and ice temperatures. Additionally, we observe ~~infrequent~~ refreezing events below 5-10 m of cold ice. Meltwater is likely moving to that depth through subsurface fractures that are not obviously visible at the surface.

In analyzing a series of processes that control near-surface ice temperature, we find that some lead to colder ice, and others to warmer, but most are strong enough to dramatically alter the ice temperature from the purely diffusive case. With rapid ablation, a spatially variable temperature field, and subsurface refreezing events, T_0 in the ablation zone should not be expected to match the air temperature. That our measurements are consistently warmer, could simply be due to the limited number of observations we have, but latent heat additions are clearly measured and could be common in near-surface ice of the western Greenland ablation zone.

References

Alley, R. B., Dupont, T. K., Parizek, B. R., & Anandakrishnan, S. (2005). Access of surface meltwater to beds of sub-freezing glaciers: Preliminary insights. *Annals of Glaciology*, 40, 8–14.
<https://doi.org/10.3189/172756405781813483>

van As, D., Hubbard, A. L., Hasholt, B., Mikkelsen, A. B., van den Broeke, M. R., & Fausto, R. S. (2012). Large surface meltwater discharge from the Kangerlussuaq sector of the Greenland ice sheet during the record-warm year 2010 explained by detailed energy balance observations. *The Cryosphere*, 6(1), 199–209.

<https://doi.org/10.5194/tc-6-199-2012>

Aschwanden, A., Bueler, E., Khroulev, C., & Blatter, H. (2012). An enthalpy formulation for glaciers and ice sheets. *Journal of Glaciology*, 58(209), 441–457. <https://doi.org/10.3189/2012JoG11J088>

Brandt, R., & Warren, S. (1993). Solar-heating rates and temperature profiles in Antarctica snow and ice. *Journal of Glaciology*, 39(131), 99–110.

Brinkerhoff, D. J., & Johnson, J. V. (2013). Data assimilation and prognostic whole ice sheet modelling with the variationally derived, higher order, open source, and fully parallel ice sheet model VarGlaS. *Cryosphere*, 7(4), 1161–1184. <https://doi.org/10.5194/tc-7-1161-2013>

van den Broeke, M., Smeets, P., Ettema, J., Van Der Veen, C., Van De Wal, R., & Oerlemans, J. (2008). Partitioning of melt energy and meltwater fluxes in the ablation zone of the west Greenland ice sheet. *Cryosphere*, 2, 179–189. <https://doi.org/10.5194/tc-2-179-2008>

Calonne, N., Flin, F., Morin, S., Lesaffre, B., Du Roscoat, S. R., & Geindreau, C. (2011). Numerical and experimental investigations of the effective thermal conductivity of snow. *Geophysical Research Letters*, 38(23), 1–6. <https://doi.org/10.1029/2011GL049234>

Carslaw, H. S., & Jaeger, J. C. (1959). *Conduction of Heat in Solids* (Second). London: Oxford University Press.

Cooper, M. G., Smith, L. C., Rennermalm, A. K., Mige, C., Pitcher, L. H., Ryan, J. C., ... Cooley, S. W. (2018). Meltwater storage in low-density near-surface bare ice in the Greenland ice sheet ablation zone. *Cryosphere*, 12(3), 955–970. <https://doi.org/10.5194/tc-12-955-2018>

Cox, C., Humphrey, N., & Harper, J. (2015). Quantifying meltwater refreezing along a transect of sites on the Greenland ice sheet. *The Cryosphere*, 9, 691–701. <https://doi.org/10.5194/tc-9-691-2015>

Cuffey, K., & Paterson, W. S. B. (2010). *The Physics of Glaciers* (Fourth). Oxford, UK: Butterworth-Heinemann.

van Everdingen, R. O. (1998). *Multi-language glossary of permafrost and related ground-ice terms*. Calgary, Alberta, CA: International Permafrost Association.

Fountain, A. G., Jacobel, R. W., Schlichting, R., & Jansson, P. (2005). Fractures as the main pathways of water flow in temperate glaciers. *Nature*, 433(7026), 618–621. <https://doi.org/10.1038/nature03296>

Harper, J. T., Humphrey, N. F., Pfeffer, W. T., Brown, J., & Fettweis, X. (2012). Greenland ice-sheet contribution to sea-level rise buffered by meltwater storage in firn. *Nature*, 491, 240–243. <https://doi.org/10.1038/nature11566>

Harrington, J. a, Humphrey, N. F., & Harper, J. T. (2015). Temperature distribution and thermal anomalies along a flowline of the Greenland Ice Sheet. *Annals of Glaciology*, 56(70), 98–104. <https://doi.org/10.3189/2015AoG70A945>

Hills, B. H., Harper, J. T., Humphrey, N. F., & Meierbacholt, T. W. (2017). Measured horizontal temperature gradients constrain heat transfer mechanisms in Greenland ice. *Geophysical Research Letters*, 44(19). <https://doi.org/10.1002/2017GL074917>

Hooke, R. L. (1976). Near-surface temperatures in the superimposed ice zone and lower part of the soaked zone of

polar ice sheets. *Journal of Glaciology*, 16(74), 302–304.

Hooke, R. L. (2005). *Principles of Glacier Mechanics* (Second). Cambridge University Press.

Hooke, R. L., Gould, J. E., & Brzozowski, J. (1983). Near-surface temperatures near and below the equilibrium line on polar and subpolar glaciers. *Zeitschrift Für Gletscherkunde Und Glazialgeologie*, 1–25.

Howat, I. M., Negrete, A., & Smith, B. E. (2014). The Greenland Ice Mapping Project (GIMP) land classification and surface elevation data sets. *Cryosphere*, 8(4), 1509–1518. <https://doi.org/10.5194/tc-8-1509-2014>

Humphrey, N. F., Harper, J. T., & Pfeffer, W. T. (2012). Thermal tracking of meltwater retention in Greenland's accumulation area. *Journal of Geophysical Research*, 117, 1–11. <https://doi.org/10.1029/2011JF002083>

Jarvis, G. T., & Clarke, G. K. C. (1974). Thermal effects of crevassing on Steele Glacier, Yukon Territory, Canada. *Journal of Glaciology*, 13(68), 243–254.

Liston, G. E., Winther, J.-G., Bruland, O., Elvehoy, H., & Sand, K. (1999). Below-surface ice melt on the coastal Antarctic ice sheet. *Journal of Glaciology*, 45(150), 273–285.

Lliboutry, L. (1965). *Traité de Glaciologie*. Paris: Masson. <https://doi.org/10.1002/qj.49709439916>

Loewe, F. (1970). Screen temperatures and 10 m temperatures. *Journal of Glaciology*, 9(56), 263–268.

Logan, J. D., & Zlotnik, V. (1995). The convection-diffusion equation with periodic boundary conditions. *Applied Mathematics Letters*, 8(3), 55–61. [https://doi.org/10.1016/0893-9659\(95\)00030-T](https://doi.org/10.1016/0893-9659(95)00030-T)

Lüthi, M. P., Ryser, C., Andrews, L. C., Catania, G. a., Funk, M., Hawley, R. L., ... Neumann, T. a. (2015). Heat sources within the Greenland Ice Sheet: dissipation, temperate paleo-firn and cryo-hydrologic warming. *The Cryosphere*, 9(1), 245–253. <https://doi.org/10.5194/tc-9-245-2015>

Lüthi, M., Funk, M., Iken, A., Gogineni, S., & Truffer, M. (2002). Mechanisms of fast flow in Jakobshavn Isbrae, West Greenland: Part III. measurements of ice deformation, temperature and cross-borehole conductivity in boreholes to the bedrock. *Journal of Glaciology*, 48(162), 369–385.

Meierbachtol, T. W., Harper, J. T., Johnson, J. V., Humphrey, N. F., & Brinkerhoff, D. J. (2015). Thermal boundary conditions on western Greenland: Observational constraints and impacts on the modeled thermomechanical state. *Journal of Geophysical Research: Earth Surface*, 120, 623–636.
<https://doi.org/10.1002/2014JF003375>. Received

Miller, N. B., Turner, D. D., Bennartz, R., Shupe, M. D., Kulie, M. S., Cadeddu, M. P., & Walden, V. P. (2013). Surface-based inversions above central Greenland. *Journal of Geophysical Research: Atmospheres*, 118(2), 495–506. <https://doi.org/10.1029/2012JD018867>

Mock, S. J., & Weeks, W. F. (1966). The distribution of 10 meter snow temperatures on the Greenland Ice Sheet. *Journal of Glaciology*, 6(43), 23–41.

Müller, F. (1976). On the thermal regime of a high-arctic valley glacier. *Journal of Glaciology*, 16(74), 119–133.

Nath, P. C., & Vaughan, D. G. (2003). Subsurface crevasse formation in glaciers and ice sheets. *Journal of Geophysical Research*, 108(B1), 1–12. <https://doi.org/10.1029/2001JB000453>

Paterson, W. S. B. (1972). Temperature distribution in the upper layers of the ablation area of Athabasca Glacier,

Alberta, Canada. *Journal of Glaciology*, 11(61), 31–41.

Paterson, W. S. B., & Savage, J. C. (1970). Excess pressure observed in a water-filled cavity in Athabasca Glacier, Canada. *Journal of Glaciology*, 9(95), 103–107.

Perovich, D. K. (2007). Light reflection and transmission by a temperate snow cover. *Journal of Glaciology*, 53(181), 201–210. <https://doi.org/10.3189/172756507782202919>

Phillips, T., Rajaram, H., Colgan, W., Steffen, K., & Abdalati, W. (2013). Evaluation of cryo-hydrologic warming as an explanation for increased ice velocities in the wet snow zone, Sermeq Avannarleq, West Greenland. *Journal of Geophysical Research: Earth Surface*, 118(3), 1241–1256. <https://doi.org/10.1002/jgrf.20079>

Phillips, T., Rajaram, H., & Steffen, K. (2010). Cryo-hydrologic warming: A potential mechanism for rapid thermal response of ice sheets. *Geophysical Research Letters*, 37(20), 1–5. <https://doi.org/10.1029/2010GL044397>

Poinar, K., Joughin, I., Lenaerts, J. T. M., & van den Broeke, M. R. (2016). Englacial latent-heat transfer has limited influence on seaward ice flux in western Greenland. *Journal of Glaciology*, 1–16. <https://doi.org/10.1017/jog.2016.103>

Tedesco, M., Fettweis, X., Mote, T., Wahr, J., Alexander, P., Box, J., & Wouters, B. (2013). Evidence and analysis of 2012 Greenland records from spaceborne observations, a regional climate model and reanalysis data. *The Cryosphere*, 7, 615–630. <https://doi.org/10.5194/tcd-6-4939-2012>

van de Wal, R. S. W., Boot, W., Smeets, C. J. P. P., Snellen, H., van den Broeke, M. R., & Oerlemans, J. (2012). Twenty-one years of mass balance observations along the K-transect, West Greenland. *Earth System Science Data*, 4(1), 31–35. <https://doi.org/10.5194/essd-4-31-2012>

Warren, S. G. (1982). Optical properties of snow. *Reviews of Geophysics*. <https://doi.org/10.1029/RG020i001p00067>

Wientjes, I. G. M., & Oerlemans, J. (2010). An explanation for the dark region in the western melt zone of the Greenland ice sheet. *Cryosphere*, 4(3), 261–268. <https://doi.org/10.5194/tc-4-261-2010>

Yen, Y.-C. (1981). *Review of thermal properties of snow, ice, and sea ice. CRREL Report 81-10*. Retrieved from <http://acwc.sdp.sirsi.net/client/search/asset/1005644>

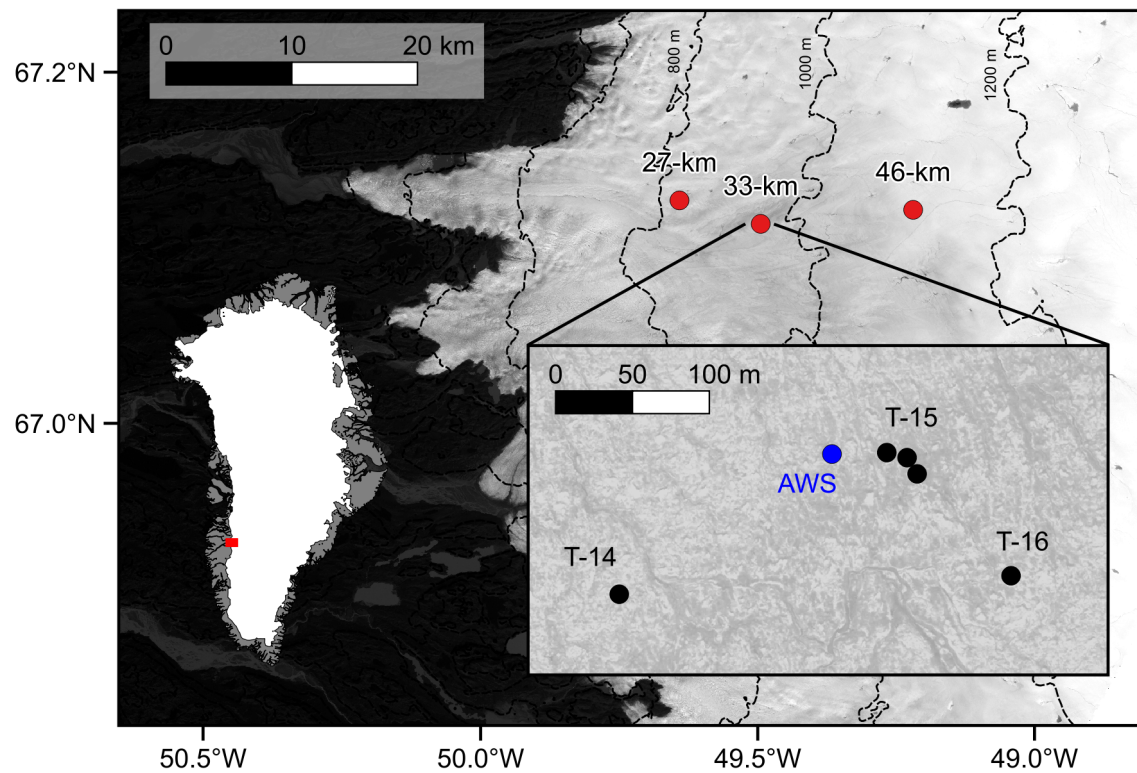


Figure 1: A site map from southwest Greenland with field sites (red) named by their location with respect to the outlet terminus of Isunnguata Sermia. The inset shows locations of near-surface temperature strings (black) named by the year they were installed and an automated weather station meteorological station (blue). Surface elevation contours are shown at 200-m spacing (Howat et al., 2014).

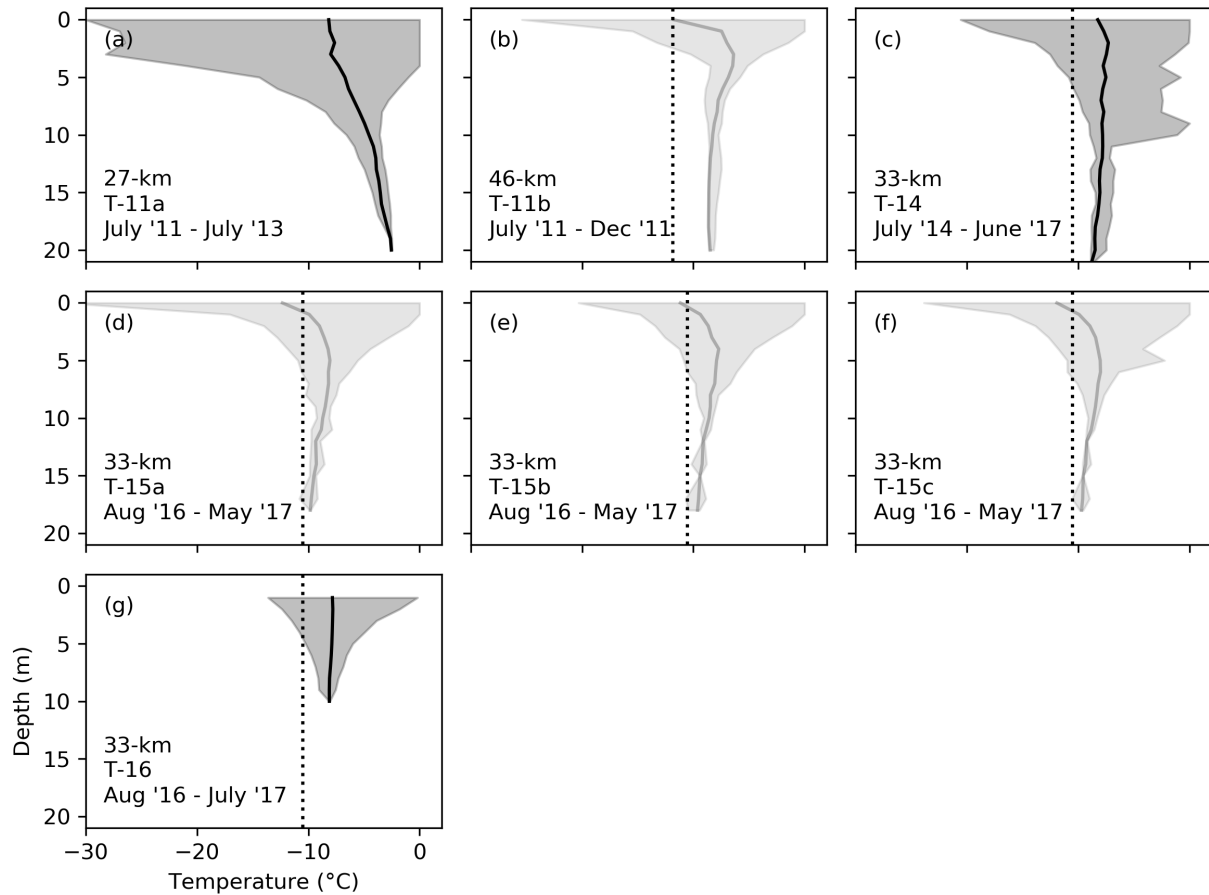


Figure 2: Near-surface ice temperature measurements from seven strings: T-11a, T-11b, [T-14](#), T-15a, T-15b, T-15c, [T-14](#), and T-16. For each, the shaded region shows the range of measured temperatures over the entire measurement period, and the [red dots](#)solid lines indicates [a-the mean value for each sensor](#)temperature profile. Depths are plotted with respect to the surface at the time of measurement, so sensor locations move toward the surface as ice melts. Strings with less than [11 months of data are slightly more transparent](#). For field sites at which the air temperature was measured for at least a full year, a dashed line shows the mean air temperature.

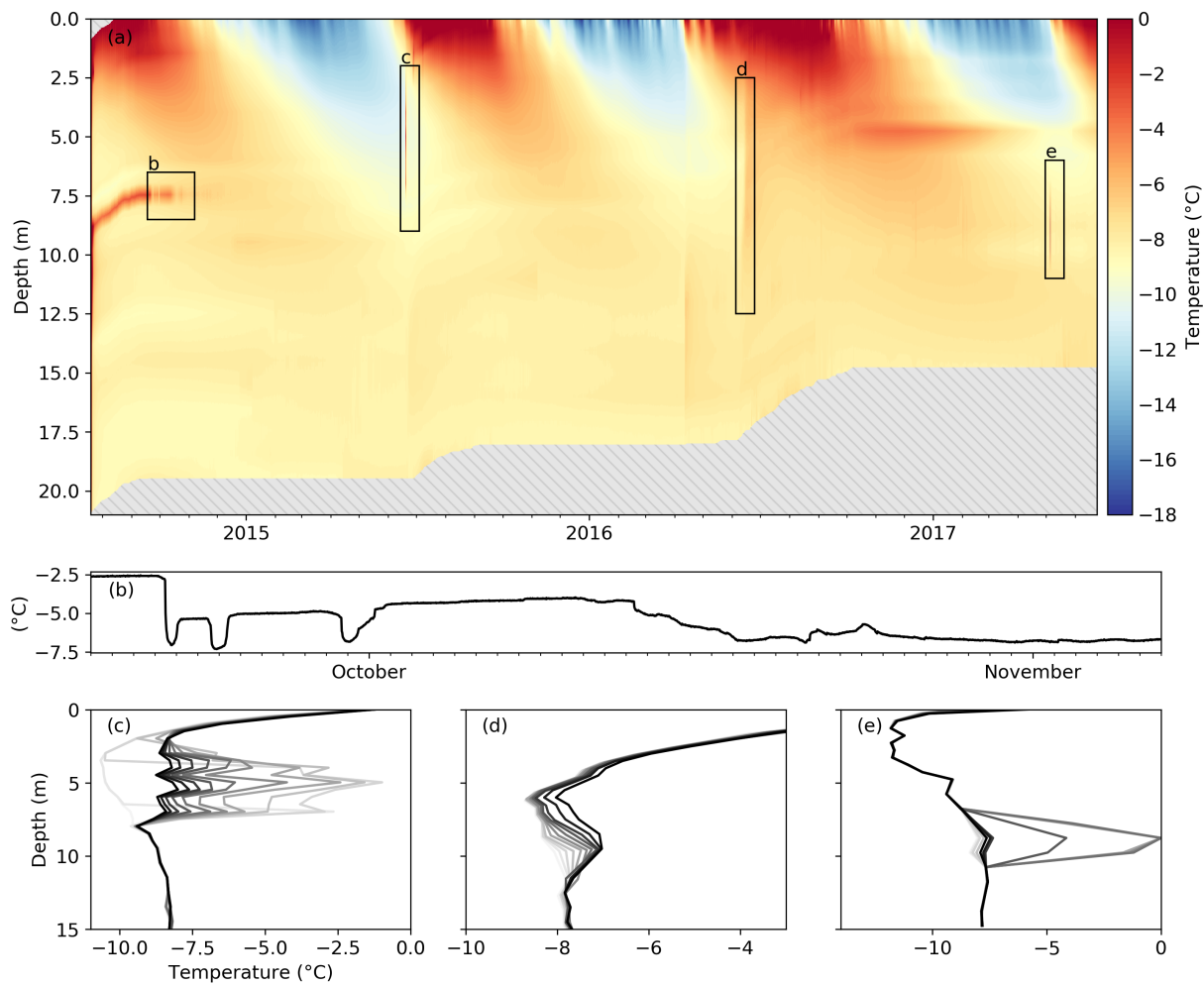


Figure 3: Three years of ice temperature measurements from the T-14 string. While this string was initially installed to 210 m depth, the sensors closest to the surface melt out as the surface drops measurements are plotted with reference to the moving surface so the sensors move up throughout the time period, revealing a gray mask. Transient features in the data include anomalously slow freeze-in behavior in one sensor (b) as well as heating events throughout the collection time period (c, d, and e). The heating events are plotted as a series of temperature profiles with the darker shades being later times and time steps between profiles of 2 hours (c), 10 hours (d), and 1 hour (e). Here, ablation measurements (corresponding to Figure 5b) are plotted as a white mask so that measurements from sensors laying at the surface are hidden.

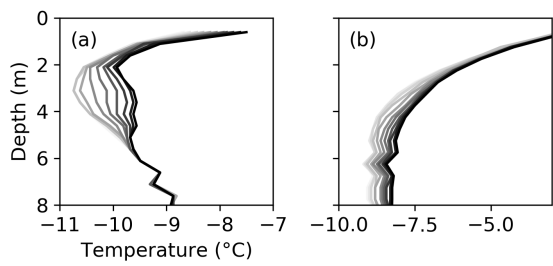


Figure 4: Heating events within the ice temperature record from two separate strings at 33 km from temperature string T-16. Profiles are plotted as in Figure 3 c, d, and e. Profiles are displayed as a series through time with lighter being earlier and darker being later. The time steps between profiles are (a) 2 hours-hour (a)s and 4 hours (b), (b) 10 hours, (c) 1 hour, and (d) 2 hours.

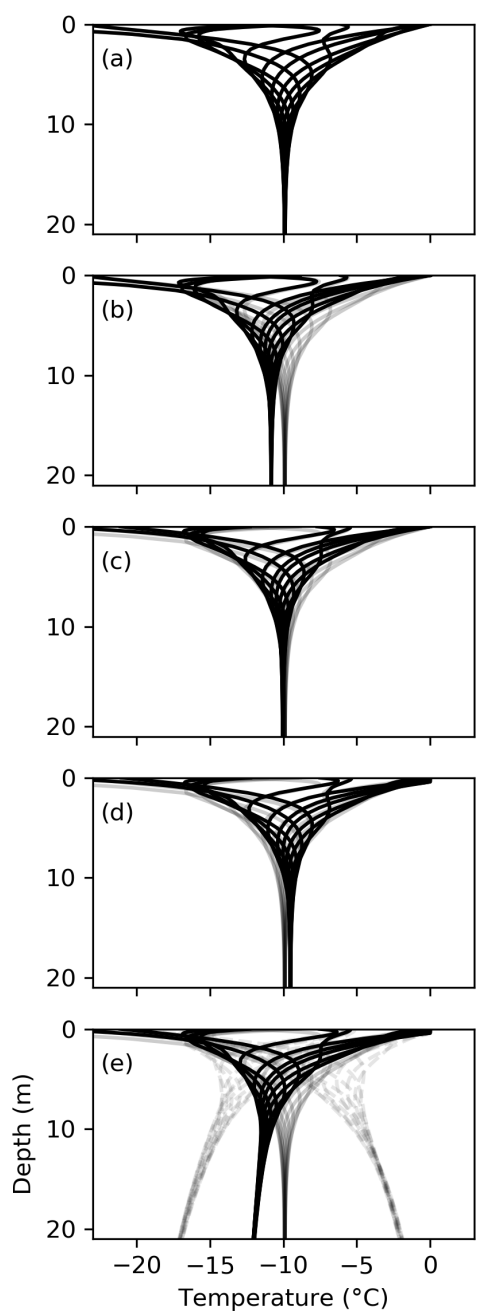


Figure 5: Meteorological data from 33 km over three years including a) air temperature, b) ice surface location, c) snow depth, and d) net shortwave radiation. All data are plotted as a daily mean. The shaded region encloses the time period that is used for the model case study.

Figure 56: Model results for ~~five~~six separate simulations. In each case, twelve simulated temperature profiles are shown from throughout the yearlong period, and control results (from (a)) are displayed for comparison (gray). Differences between the simulations are analyzed quantitatively using T_{0s} , the convergent temperature at 21 m. Processes are from top to bottom: a) control model run simulation of pure diffusion, b) ablation, c) snow insulation, d) radiative energy input, and finally e) subsurface20-m temperature gradient. The two limiting cases for the subsurface temperature gradient are plotted with dashed gray lines (e).

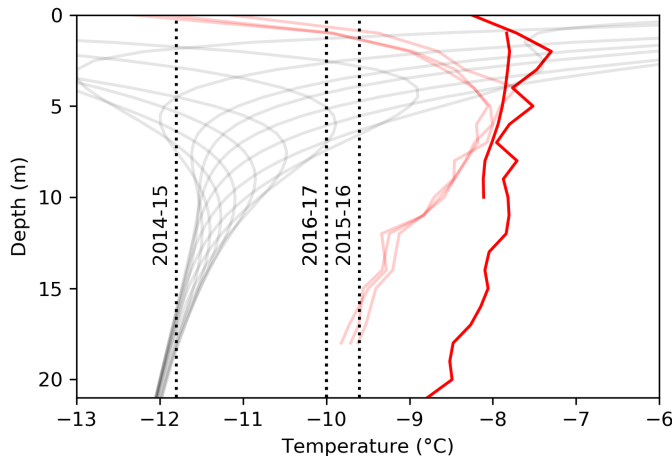


Figure 67: A comparison of model output (gray) and data from 33-km, including mean ice temperatures (red) and mean annual air temperatures for three seasons (black dashed). The observed measuredice temperatures are plotted differently from the same as in Figure 2. Instead of fixed sensor locations, the depth here is plotted at a distance relative to a melting surface (the same way as the model results). Note that three of the temperature strings failed before running for an entire year collected only ~9 months of data (transparent red). Mean temperatures from those three strings are biased cold near the surface because they collected more wintertime measurements than summertime.

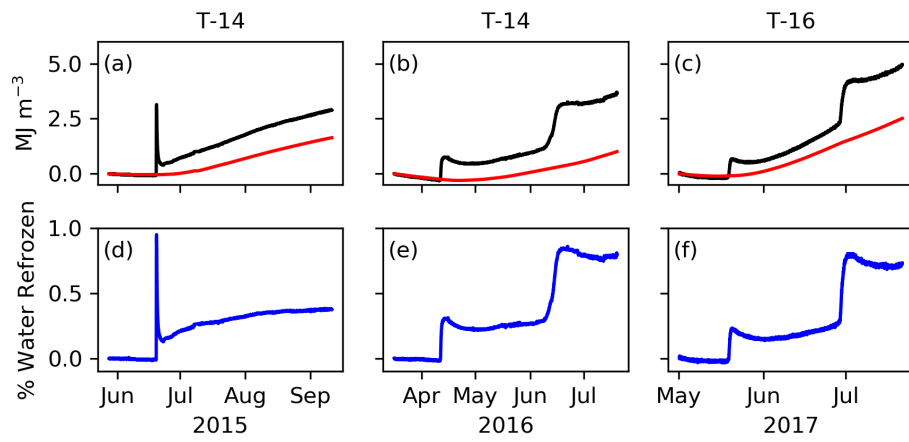


Figure 7: Energy source for the observed heating events. a-c) Observed energy density through time for the differenced temperature profile calculated with equation (9) (black), and conductive energy density through time calculated with equation (10) (red). d-f) Percent by volume water refrozen for the associated source in (a-c). This value is proportional to the difference between the black and red lines above. The temperature string from which measurements were taken is labeled at the top.

Table 1: Temperature Strings

String Name	Data Time Period	Time Step (hr)	Sensor	# of Sensors	Sensor Spacing (m)	Latitude	Longitude	Elevation (m)
T-11a	7/5/11 – 7/15/13	3	Thermistor	32	0.6	67.195175	-49.719515	848
T-11b	7/11/11 – 12/17/11	3	Thermistor	32	0.6 < 11 m deep – 0.5	67.201553	-49.289058	1095
T-14	7/18/14 – 8/14/16	0.5	Thermistor	31	> 11 m deep – 1.0 < 15 m deep – 1.0	67.18127	-49.56982	956
T-15a	08/17/16	N/A	DS18B20	17	> 15 m deep – 3.0 < 15 m deep – 1.0	67.18211	-49.568272	954
T-15b	08/17/16	N/A	DS18B20	17	> 15 m deep – 3.0 < 15 m deep – 1.0	67.182054	-49.568059	954
T-15c	08/17/16	N/A	DS18B20	17	> 15 m deep – 3.0	67.182114	-49.568484	954
T-16	08/17/16	N/A	DS18B20	18	0.5	67.18147	-49.57025	951

Table 2: Constants

Variable	Symbol	Value	Units	Reference
Reference Enthalpy	H_m	0	J kg^{-1}	
Ice Density	ρ_i	917	kg m^{-3}	Cuffey and Paterson (2010)
Snow Density	ρ_s	300	kg m^{-3}	
Water Density	ρ_w	1000	kg m^{-3}	
Specific Heat Capacity	C_p	2097	$\text{J kg}^{-1} \text{K}^{-1}$	Cuffey and Paterson (2010)
Latent Heat of Fusion	L_f	3.335×10^5	J kg^{-1}	Cuffey and Paterson (2010)
Thermal Conductivity of Ice	k_i	2.1	$\text{J m}^{-1} \text{K}^{-1} \text{s}^{-1}$	Cuffey and Paterson (2010)
Thermal Conductivity of Snow	k_s	0.2	$\text{J m}^{-1} \text{K}^{-1} \text{s}^{-1}$	Calonne et al. (2011)
Moisture Diffusivity	ν	1×10^{-4}	$\text{kg m}^{-1} \text{s}^{-1}$	Aschwanden et al. (2012)